2016 IEEE 55th Conference on Decision and Control (CDC)
ARIA Resort & Casino
December 12-14, 2016, Las Vegas, USA

3D Multi-Contact Gait Design for Prostheses: Hybrid System Models, Virtual Constraints and Two-Step Direct Collocation

Huihua Zhao[1], Ayonga Hereid[1], Eric Ambrose[1] and Aaron D. Ames[2]

Abstract— **Virtual constraints have been recognized as an essential bridging tool which has the potential to translate rich nonlinear bipedal control methodologies to the control of prostheses. In this paper, we propose a hybrid system model based two-step direct collocation approach to automatically generate three-dimensional (3D) human-like multi-contact prosthetic gaits (via virtual constraints) for an asymmetric amputee-prosthesis system model. Unimpaired human locomotion is studied first to provide a reference for this gait design method. Specific requirements—such as amputee comfortability, human-likeness, physical limitations for hardware implementation—are then discussed explicitly in order to quantify a well-designed prosthetic gait. A 29 degrees of freedom 3D unsymmetrical bipedal robotic model is considered to model the asymmetric amputee-prosthesis system. Imposing the prosthetic gait requirements as nonlinear constraints and utilizing the asymmetric 3D hybrid system model, a two-step direct collocation based optimization method is proposed to generate 3D prosthetic gaits automatically. The resulting prosthetic gait is analyzed in detail, showing the designed multi-contact gait is human-like, formally stable and optimal w.r.t the requirements.**

I. INTRODUCTION

Amputees with energetically passive prosthetic devices are found to be less stable, constrained in locomotion capabilities and require more force and energy during locomotion than healthy humans [9], [29]. Powered-lower-limb prostheses capable of providing net power in conjunction with various prostheses controllers have been developed in recent decades with the potential to regain full mobility in various terrains for amputees. For example, [10] developed a hydraulically actuated knee prosthesis with the "echo control" method to mirror the modified trajectory of a healthy leg on the opposing side. Gait-pattern generator based controllers have been successfully realized on prostheses [21]. Among these different prostheses controllers, variable impedance control is one of the most common approaches for controlling prostheses (to name a few [6], [16], [24], [25]). In particular, this control method breaks one step cycle into multiple phases, each of which has its own impedance parameters along with the corresponding phase switching parameters. Currently clinicians tune these parameters by trial and error for each patient [25]. This impedance controller tuning process takes four hours on average for each individual as mentioned in [24]. Moreover, multiple sessions are necessary to tune the device for different modes of locomotion such as stair ascent/descent and ramp ascent/descent.

On the other end of the spectrum, as motivated by the control of bipedal walking robots, virtual constraints (which are imposed by motor actuators as opposite to physical constraints) can be utilized to design a unified reference prosthetic gait for tracking purposes [26]. Compared to the traditional impedance control, this method has several advantages: a) it does not require discretization of a step cycle, therefore, eliminating possible incidents of incorrect phase switching; b) stability can be formalized and analyzed mathematically; c) optimal nonlinear controllers can be applied potentially to reduce parameter-tuning and improve energy performance. Motivated by these benefits, multiple past results have successfully implemented this method with achieving prosthetic walking in either simulation or experiment. Control of a powered prosthetic leg through virtual constraints using the Center of Pressure (COP) as a phasing variable was realized in [11]. Adaptive control is utilized to track a predefined trajectory with realizing robust prosthetic walking on a prosthesis test robot in [7]. Feedback decentralized controllers are utilized with achieving exponentially stable 3D prosthetic walking in simulation [14].

Previous work of the authors have shown a systematic methodology of transferring the framework of human-inspired control and optimization, which has proven success on bipedal walking robots [3], [30], to automatically generate prosthetic gaits aiming to reduce the effort of parameter tuning. Combining this optimization method with a real-time control Lyapunov function based quadratic programming controller [4], the resulting stable prosthetic walking is human-like both kinetically and kinematically [31]. Additionally, the proposed nonlinear controller (tested for both flat ground walking [31] and walking upstairs [33]) has shown improved tracking performance while at the same time requiring less energy (compared to PD control). Despite the improvements achieved by the framework of virtual constraints, the previous results were still limited by several basic assumptions: a) forward human walking is simplified as a 2D model; b) the amputee-prosthesis system is assumed to be symmetric; c) realistic requirements (human comfortability, energy consumption, hardware torque and velocity limitations) of a prosthetic gait have not yet been considered intuitively during the gait design procedure.

This research is supported by NSF CAREER Award CNS-0953823.

[1]H. Zhao, A. Hereid and E. Ambrose are with Mechanical Engineering, Georgia Institute of Technology, Atlanta, USA. {huihua, ayonga, eamborse}@gatech.edu

[2]Prof. A. Ames is with department of Mechanical Engineering and Electrical Engineering, Georgia Institute of Technology, Atlanta, USA. ames@gatech.edu

The main objective of this paper is to solve these problems by proposing a novel two-step asymmetric 3D virtual constraints design method for generating human-like multi-contact prosthetic gaits, which also satisfy various realistic requirements such as human comfortability and energy consumption. Beginning with the analysis of both unimpaired human locomotion and the special case of amputee walking, explicit requirements of a well-designed prosthetic gait are discussed in Sec. II, which forms the design objectives of this work. With the goal of fully capturing the essentials of human locomotion, a 3D bipedal hybrid system model is developed to characterize the asymmetric multi-contact amputee-prosthesis locomotion system in Sec. III. Two springy feet with high stiffness passive springs are included in the model to capture effects of compliance in both the human and prosthetic foot. A Lagrangian system combined with holonomic constraints is utilized to model the continuous dynamics of both the amputee and prosthesis separately. The two subsystems are then connected using a virtual socket to form a complete bipedal robot model.

The system asymmetries considered in this work include several aspects, such as different mass and inertia properties. More importantly, during the process of gait design, specific requirements on both human comfortability and hardware implementation need to be considered for the prosthetic leg. Imposing the requirements as constraints and objectives, a two-step direct collocation method is proposed to design human-like prosthetic gaits for this asymmetric 3D model in Sec. IV. Finally, in Sec. V, the resulting prosthetic gait is studied in detail in simulation, showing that a natural human-like amputee-prosthesis walking is achieved that fulfills the requirements of a "well-designed" prosthetic gait.

II. PROSTHETIC GAIT DESIGN

The ultimate goal of a powered prostheses controller is to recover motion abilities of amputee subjects. The resulting prosthetic walking as discussed in [22] should: a) look as close to healthy human walking as possible (human-likeness requirement); b) interact with amputee subjects naturally without exerting undesirable forces or torques (comfortability requirement); c) be torque optimal to bear the human weight and at the same time be energy efficient (physical limitation requirement). Bearing these objectives in mind, this section begins with reviewing the multi-domain behavior embedded in human locomotion [2], [5], [30]. The detailed performance requirements of a "well-designed" prosthetic gait are then discussed explicitly in this section.

A. Multi-Contact Human Locomotion

During the course of a step, humans undergo changes in phase through changes in their contact points with the environment (heel or toe leaving and striking the ground) as depicted in Fig. 1. This multi-domain, or multi-contact nature of the human gait results in walking which is both fluid and efficient [17]. Using the foot push off during the single support phase, a human can lift the swing leg higher, and thus achieve greater foot clearance without bending the swing knee significantly. By having the body pivoting over the the stance toe, much less energy is required for a human to move forward through the utilization of their forward rotational momentum. Researchers also found that the prosthetic foot push off is negatively correlated with leading intact limb loading impulse, which may help reduce knee osteoarthritis in lower extremity amputees [19]. Therefore, incorporating these advantages into prostheses locomotion in a systematic way is important for truly human-like prosthetic walking both kinetically and kinematically [31].

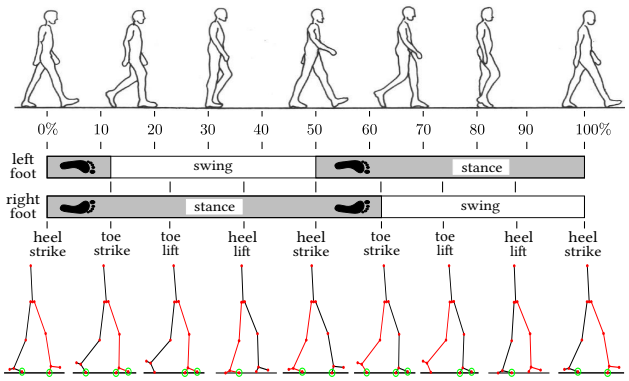

Fig. 1: Multi-contact locomotion diagram of a typical human gait cycle [2] (top) and multi-contact domain breakdown of two steps of one subject based on the changes of heel and toe contact condition (bottom). Green circle represents one specific point is in contact with the walking surface.

With the goal of formally constructing this multi-contact feature for later use of prosthetic gait design, we break one step cycle into sub-phases based on the contact points of heel and toe. In particular, utilizing the acceleration-based domain breakdown method discussed in [32], it is found that human locomotion can be divided into four domains (i.e., sub-phases) in general [5], [32], which are termed based on the switching event of that domain as toe-strike (ts), toe-lift (tl), heel-lift (hl) and heel-strike (hs). The domain breakdown of one subject is plotted in Fig. 1 along with the triggering events to show the domain configuration explicitly. As it is essential to recognize that human gait can be assumed to be a cyclic motion, we will use this four-domain cycle to characterize one stride during amputee-prosthesis walking.

B. Performance Requirements for Prostheses Gait Design

Based on the general requirements of prostheses controllers as discussed above, we explicitly consider the following three groups of performance requirements for prosthetic gait design purposes in this work.

"Human-likeness" Requirements. The first term of human-likeness requirements we consider is *similarity to unimpaired walking*, which has been previously used in [6], [25]. Motivated by the fact that humans share a common joint pattern during locomoting [29], a nominal human trajectory can be utilized as a reference for this gait design method. We quantify this term by finding the coefficient of determination (R^2) between the resulting prosthetic knee and ankle tra-

jectories, and nominal unimpaired trajectories. Additionally, the *measure of symmetry* between the prosthetic leg and the amputee's unimpaired leg is also evaluated as one of the "human-likeness" constraints [18].

Comfortability Requirements. The undesired pressure of amputee-prosthesis system mostly come from the socket adapters during the stance phase and the unprepared landing when the prosthetic leg strikes the ground [9]. Therefore, the first term we considered for this group is the *reaction wrenches* exerted in the connection socket between the prosthetic leg and amputee subject. While there is no reference about a realistic optimal value, we believe that lower values are positively related to better user experiences with the condition that prosthetic devices can still perform safely.

Velocity matching has been a known term in bipedal robotics aiming to reduce impact forces. As proper landing velocity could potentially reduce uncomfortable forces exerted from the socket, we consider the absolute *impact heel velocity* of the prosthetic leg as the second term of the comfortability requirements.

Physical Limitation Requirements. Powered-prosthetic devices are required to be light-weight and compact, therefore, yielding hardware limitations on various levels. For example, the maximum applicable torques and velocities are limited by the size of the motor and the transmission systems. Operation duration (i.e., actively walking time) is limited by the battery pack, the size and weight of which are a big concern during the prosthetic hardware design. In particular, we consider the objective to be the *mechanical cost of transport* (CoT) as defined $\Phi_{CoT} = P_{total}/(W*v)$, where P is the total mechanical power, W is the subject weight and v is the average forward velocity during one complete step cycle [8]. Additionally, to guarantee that the designed gaits are feasible for implementation on hardware devices, *maximum torques* and *maximum velocities* are considered as the other two terms of physical requirements.

III. MODEL OF AMPUTEE-PROSTHESIS SYSTEM

Human locomotion is recognized to be cyclic with domains transitioning in an ordered and periodic manner. This motivates the use of a multi-domain hybrid system with a predetermined ordering of phases (or domains) as represented by a cyclic directed graph [5], [30]. Formally, the definition of a *multi-domain hybrid control system* is given as a tuple (see [5] for a full definition),

$$\mathscr{HC} = (\Gamma, \mathscr{D}, \mathscr{U}, S, \Delta, FG), \tag{1}$$

where $\Gamma = (V, E)$ is a directed cycle. In this section, we briefly introduce remaining elements of the hybrid system model. For simplicity of notation, we specify $v \in V$ be an arbitrary vertex, v^+ be the subsequent vertex of v in the cycle, and $e = \{v \to v^+\}$ be the transition from v to v^+ for the remainder of the paper.

A. Dynamics of Amputee-Prosthesis System

An amputee-prosthesis system is an asymmetric system with two legs (one unimpaired leg and one prosthetic leg) having different properties in various aspects. For example, the two legs have different mass and inertia properties. The movement range and feasible torques are also different. These differences motivate us to model the amputee part and prosthetic leg separately.

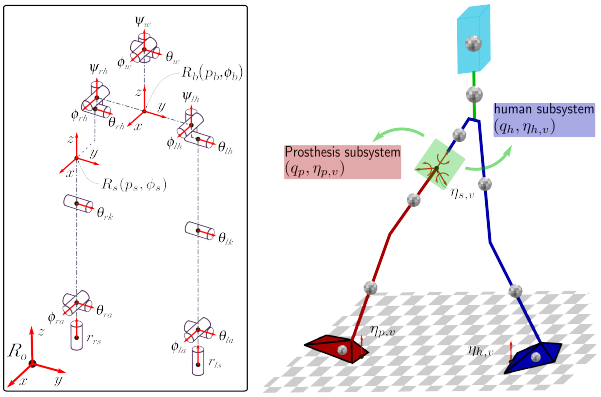

Fig. 2: Model of Amputee-Prosthesis System

Continuous Dynamics of Amputee. The amputee (or human) sub-system is modeled as a kinematic chain with an inertial reference frame $R_b = \{p_b, \varphi_b\} \subset \mathbb{R}^6$ attached at the center of the hip as shown in Fig. 2. As illustrated in the left plot of Fig. 2, the kinematic chain of body coordinates consists of three branches: waist joints $q_w = [\psi_w, \varphi_w, \theta_w]^T$, left leg (which is assumed to be the unimpaired leg) joints $q_l = [\psi_{lh}, \varphi_{lh}, \theta_{lh}, \theta_{lk}, \theta_{la}, \varphi_{la}, r_{ls}]^T$ and the right amputated hip $q_{rh} = [\psi_{rh}, \varphi_{rh}, \theta_{rh}]^T$, respectively. Therefore, we define the configuration space of the human sub-system as $\mathscr{Q}_h$: $q_h = \{R_b, q_w, q_l, q_{rh}\} \subset \mathbb{R}^{19}$ with 13 degrees of actuation (6 actuators at the two hips, 3 at the waist, 1 at the knee and 2 at the ankle). Note that, we model the rubber shoes as stiff passive spring ($k_{stiffness} = 60000N/m, b_{damping} = 600Ns/m$) on both legs as a prismatic joint to better capture the compliance characteristics of both the human sole and springy prosthetic foot [13]. With the anthropomorphic mass, inertia and length properties of each link estimated based on the method in [29] of a real subject, the equation of motion (EOM) for a given domain $\mathscr{D}_v$ is determined by the Euler-Lagrange equation [12], [20]:

$$D_h(q_h)\ddot{q}_h + H_h(q_h, \dot{q}_h) = B_{h,v}u_{h,v} + J_{h,v}^T(q_h)F_{h,v}, \tag{2}$$

where $F_{h,v} : T\mathscr{Q}_h \times U_{h,v} \to \mathbb{R}^{n_{h,v}}$, with $n_{h,v}$ the number of total holonomic constraints, is a vector of contact *wrenches* containing the constraint forces and/or moments (see [20]). $J_{h,v}$ is the corresponding Jacobian matrix of the contact points (i.e., holonomic constraints set denoted as $\eta_{h,v}$) of the amputee in domain v. To enforce the holonomic constraints, the second order differentiation of the constraints, $\eta_{h,v}$ should be set to zero,

$$J_{h,v}(q_h)\ddot{q}_h + \dot{J}_{h,v}(q_h, \dot{q}_h)\dot{q}_h = 0. \tag{3}$$

The constrained dynamics of the system is determined by evaluating both (2) and (3) simultaneously.

Continuous Dynamics of Prosthesis. The similar method is used to model the prosthesis sub-system. Considering

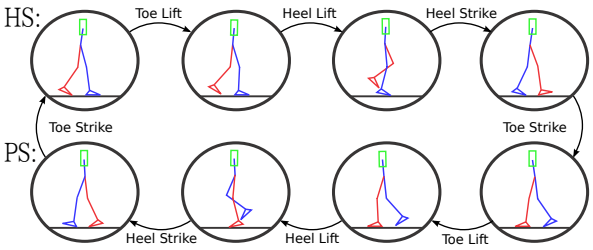

Fig. 3: Two-step domain graph of the asymmetric amputee-prosthesis gait.

the fact that the prosthetic device will be connected to the amputee at the amputated thigh by using a socket adapter, we choose base frame for prosthesis leg $R_s = \{p_s, \varphi_s\} \subset \mathbb{R}^6$ at the place where the socket adapter is, which is shown in Fig. 2. The prosthetic leg has 4 degrees of freedom $q_{rp} = [\theta_{rk}, \theta_{ra}, \varphi_{ra}, r_{rs}]^T$ and actuated at the joints of knee pitch, ankle pitch and ankle roll. With configuration space $\mathscr{Q}_p$: $q_p = \{R_s, q_{rp}\} \subset \mathbb{R}^{10}$ and mass, inertial properties obtained from the design of prostheses, the dynamics can be given as:

$$D_p(q_p)\ddot{q}_p + H_p(q_p, \dot{q}_p) = B_{p,v}u_{p,v} + J_{p,v}^T(q_p)F_{p,v}, \quad (4)$$

$$J_{p,v}(q_p)\ddot{q}_p + \dot{J}_{p,v}(q_p, \dot{q}_p)\dot{q}_p = 0, \quad (5)$$

where $F_{p,v} : T\mathscr{Q}_p \times U_{p,v} \to \mathbb{R}^{n_{p,v}}$, with $n_{p,v}$ the number of total holonomic constraints of the prosthetic device. The rest of the terms are defined similarly as (2) and (3).

Combined Bipedal Amputee-Prosthesis System. With the dynamics of both the amputee and prosthesis in hand, we are now ready to connect these two sub-systems into a complete bipedal model via enforcing holonomic constraints at the socket. Particularly, for the combined bipedal system, the configuration space can be defined as $\mathscr{Q} : q = \{q_h, q_p\} \subset \mathbb{R}^{29}$; holonomic constraints are grouped as $\eta_v = \{\eta_{h,v}, \eta_{p,v}, \eta_{s,v}\}$ (corresponding to $F_v = \{F_{h,v}, F_{p,v}, F_{s,v}\}$) with $\eta_{s,v}$ ($F_{s,v}$) is the set of holonomic constraints imposed by the socket. Therefore, based on the new complete coordinates, the general dynamics for $\mathscr{D}_v$ can be given as:

$$D(q)\ddot{q} + H(q, \dot{q}) = B_v u_v + J_v^T(q)F_v, \quad (6)$$

$$J_v(q)\ddot{q} + \dot{J}_v(q, \dot{q})\dot{q} = 0. \quad (7)$$

Due to this asymmetric model construction, one human stance step (HS) and one prosthesis stance step (PS) are necessary to form a complete two-step cycle, therefore, resulting a directed graph with 8 domains as shown in Fig. 3. For notation simplicity, we name each domain with a combination of the stance leg type and domain trigger type (e.g., *hs* or *tl*). For example, the heel strike domain during PS phase is notated as *phs*. Therefore, the directed graph Γ can be explicitly stated as $V = \{htl, hhl, hhs, hts, ptl, phl, phs, pts\}$ and the edges E are the corresponding triggering events. With notation $x = (q; \dot{q})$, the affine control system for each domain $\mathscr{D}_v$ can be obtained as $\dot{x} = f_v(x) + g_v(x)u_v$ by reformulating (6) and (7) [28]. The discrete behavior, Δ_e, of impacts is modeled with the assumption of perfectly plastic impacts. More details can be found in [28].

B. Virtual Constraints

Analogous to holonomic constraints that are imposed by physical contact conditions, virtual constraints (also termed *outputs* in [3]) are defined as a set of functions that modulate the behavior of a robot in order to achieve certain desired trajectories [28]. Mathematically, virtual constraints are defined as the difference between the actual and desired outputs of the robot system:

$$y_{1,v}(q, \dot{q}) = \dot{y}_{1,v}^a(q, \dot{q}) - y_{1,v}^d(\alpha_v), \quad (8)$$

$$y_{2,v}(q) = y_{2,v}^a(q) - y_{2,v}^d(\tau(q), \alpha_v), \quad (9)$$

for $v \in V$, where $y_{1,v}$ and $y_{2,v}$ are relative degree 1 and (vector) relative degree 2 outputs by definition (see [23] for the definition of relative degree), respectively. Specifically, we assume the desired velocity-modulating output to be a constant, i.e., $y_{1,v}^d(\alpha_v) = v_d \in \mathbb{R}$ and the desired position-modulating outputs are given in term of a Bézier polynomial of degree M, determined by $M+1$ coefficients [28]:

$$y_2^d(\tau, \alpha_o) := \sum_{k=0}^{M} \alpha_o[k] \frac{M!}{k!(M-k)!} \tau^k (1-\tau)^{M-k}, \quad (10)$$

for all $o \in \mathscr{O}_v$ with $\mathscr{O}_v$ be an indexing set of outputs, and α_o is a vector of Bézier polynomial coefficients. Note that, the explicit discussion of outputs set for each domain is omitted here as the major focus of this work are the ankle and knee joints. The phase variable, $\tau(q)$, which has to be monotonic over a gait cycle, is introduced aiming to create a robust autonomous controller as discussed in [28].

Partial Hybrid Zero Dynamics. The feedback linearization control law described in Eq. 28 of [3] can drive the virtual constraints $y_v = (y_{1,v}, y_{2,v}) \to 0$ exponentially. However, $y_v \to 0$ is not necessarily invariant through discrete dynamics. With relaxing the invariance of the relative degree 1 output (considering the changes of velocity at impact), we enforce conditions only related to the relative degree 2 virtual constraints, $y_{2,v}$, resulting in the *partial zero dynamics* surface (see [3]), given by:

$$\mathbf{PZ}_v = \{(q, \dot{q}) \in \mathscr{D}_v | y_{2,v}(q) = 0, \dot{y}_{2,v}(q, \dot{q}) = 0\}. \quad (11)$$

Moreover, for any $e \in E$, the submanifold $\mathbf{PZ}_v$ is called impact invariant, if there exist a set of parameters v_d and $\{\alpha_v\}_{v \in V}$, with $\alpha_v = (\alpha_o)_{o \in \mathscr{O}_v}$, so that

$$\Delta_e(x) \in \mathbf{PZ}_{v^+}, \qquad \forall\, x \in S_e \cap \mathbf{PZ}_v. \quad (12)$$

A manifold $\mathbf{PZ} = \bigcup_{v \in V} \mathbf{PZ}_v$ is called *hybrid invariant* if it is invariant over all domains of continuous dynamics and impact invariant through all discrete dynamics, i.e., solutions that start in $\mathbf{PZ}$ remain in $\mathbf{PZ}$, even after impulse effects. If a feedback control law renders $\mathbf{PZ}$ hybrid invariant, then we say that the multi-domain hybrid control system has a *partial hybrid zero dynamics* (PHZD), $\mathscr{H}|_{\mathbf{PZ}}$.

IV. TWO-STEP MULTI-CONTACT OPTIMIZATION

In this section, we emphasis the computationally effective nonlinear optimization that generates periodic two-step asymmetric amputee-prosthesis gaits subject to particular

requirements discussed in Sec. II. In particular, the goal is to determine a set of virtual constraints parameters v_d and $\{\alpha_v\}_{v\in V}$ so that the resulting gait satisfies the *partial hybrid zero dynamics* condition.

A. Two-Step Direct Collocation Optimization

A periodic two-step gait cycle of the amputee-prosthesis walking consists of 8 continuous domains in the order shown in Fig. 3. Using traditional single shooting optimization introduced in [30] would be extremely difficult to numerically generate optimal gaits for such a system. Therefore, we apply the direct collocation based multi-domain HZD gait design approach introduced in [15] with particular modifications for the two-step hybrid system.

Here, we simply introduce the main idea of the direct collocation optimization. In particular, the solution of each domain, $\mathscr{D}_v$, is discretized based on the time discretization

$$0 = t_0 < t_1 < t_2 < \cdots < t_{N_v} = T_{I,v}, \tag{13}$$

assuming $T_{I,v} > 0$ is the time at which the system reaches the guard associated with a given domain. Let x^i and $\dot{x}^i$ be the approximated states and first order derivatives at node i, the defect constraints are defined at each odd node as:

$$\dot{x}^i - 3(x^{i+1} - x^{i-1})/2\Delta t_v^i + (\dot{x}^{i-1} + \dot{x}^{i+1})/4 = 0, \tag{14}$$

$$x^i - (x^{i+1} + x^{i-1})/2 - \Delta t_v^i(\dot{x}^{i-1} - \dot{x}^{i+1})/8 = 0, \tag{15}$$

where $\Delta t_v^i = t_{i+1} - t_{i-1}$ is the time interval. Moreover, the first order derivatives must satisfy the system dynamics, i.e., $\dot{x}^i = f_v(x^i) + g_v(x^i)u_v^i$. The control inputs u_v^i at each node is enforced to be the feedback linearization controllers discussed in Sec. III. Further, the domain admissible constraints and guard condition are also imposed accordingly. The system states between two continuous domains are connected by enforcing the discrete dynamics, Δ_e, of each associated edge.

Followed from the general construction of the multi-domain HZD gait optimization in [15], we state the two-step amputee-prosthesis gait optimization to minimize the mechanical CoT of the gait, given as:

$$\underset{\mathbf{z}^*}{\operatorname{argmin}}\ \Phi_{CoT}(\mathbf{z}) \tag{16}$$

$$\text{s.t} \quad \mathbf{z}_{\min} \le \mathbf{z} \le \mathbf{z}_{\max}, \tag{17}$$

$$\mathbf{c}_{\min} \le \mathbf{c}(\mathbf{z}) \le \mathbf{c}_{\max}, \tag{18}$$

where $\mathbf{z}$ is the set of all decision variables, and $\mathbf{c}(\mathbf{z})$ is a collection of necessary constraints presented in [15]. In the case of two-step gait optimization, the parameters consistency constraints are enforced between domains of one step. Due to the page limit, we omit the detailed construction of the optimization in this paper. For more details, we refer the readers to [15].

B. Prosthetic Gait Design Constraints

Based on the general HZD gait optimization in (16), we primarily focus on specific performance requirements of the amputee-prosthesis gaits discussed in Sec. II-B.

Human-likeness Constraints. With the goal of designing human-like prosthetic gaits, we put a strong focus on the ankle and knee joints via constraining the differences between the optimized trajectories and the reference unimpaired walking trajectories to be bounded. Let $\theta_p^i = (\theta_{ra}^i, \theta_{rk}^i)$ be the prosthesis joint angles and $\theta_h^i = (\theta_{la}^i, \theta_{lk}^i)$ be the amputee joint angles at node i, then for two positive constants $\delta_p > 0$ and $\delta_h > 0$, we impose the *human-likeness* constraints as:

$$\|\theta_r(\tau(q^i)) - \theta_p^i\| \le \delta_p, \qquad \text{(Gait Similarity)}$$

$$\|\theta_r(\tau(q^i)) - \theta_h^i\| \le \delta_h, \qquad \text{(Gait Symmetry)}$$

where θ_r is the reference ankle and knee tranjectories that scaled on the interval of $[0,1]$ and then interpolated by the phase variable, τ. As (Gait Similarity) constrains the prosthetic trajectory to be human-like, (Gait Symmetry) guarantees the amputee trajectory is also close to the reference trajectory, therefore resulting in gait symmetry.

Comfortability Constraints. As discussed in Sec. II-B, two comfortability constraints—reaction wrenches at the socket adapter and impact velocities at the heel—are considered in our two-step gait optimization. To impose these requirements, we consider admissible boundary sets $\{F_{s,v}^{\min}, F_{s,v}^{\max}\}$ with $v \in V$ and $\{v_{hhs}^{min}, v_{hhs}^{max}\}$ for each of them. Note that, the boundaries of reaction wrenches will be different depending on the specific domain $v \in V$, therefore, we consider connection wrench constraints in a general form as:

$$F_{s,v}^{\min} \le F_{s,v}^i \le F_{s,v}^{\max}. \qquad \text{(Connection Wrench)}$$

In addition, the heel impact velocity constraints in all x, y, and z directions are imposed at the end of the human-stance heel strike domain (*hhs*) with $i = N$, which is given as:

$$v_{hhs}^{\min} \le \dot{p}_{rh}(q^N, \dot{q}^N) \le v_{hhs}^{\max}. \qquad \text{(Impact Velocity)}$$

where $p_{rh}(q)$ is the three dimensional Cartesian position the prosthesis heel (i.e., right heel).

Physical Limitation Constraints. Considering that we define the cost function of the gait optimization as the mechanical cost of transport, we are only required to apply constraints for the admissible joint torques, $u_j^{\max}$, and admissible velocities, $\dot{\theta}_j^{\max}$ which are introduced by the prosthetic hardware limitations. Hence, at each node i for all domains, we have:

$$-u_j^{\max} \le u_j^i \le u_j^{\max}, \qquad \text{(Admissible Torque)}$$

$$-\dot{q}_j^{\max} \le \dot{q}_j^i \le \dot{q}_j^{\max}. \qquad \text{(Admissible Velocity)}$$

In addition to the major constraints discussed above, other auxiliary constraints (for example, foot clearance, step length and step width) are also considered in this optimization. Due to the discretization of states and the particular defect variables formulation, all of these constraints can be directly applied on the boundary values of corresponding decision variables or the functions of the decision variables. Incorporating the above constraints in (16), the end result is a large-scale nonlinear programming (NLP) problem with over $40,000$ optimization variables and $40,000$ constraints, which can be solved in 20 minutes.

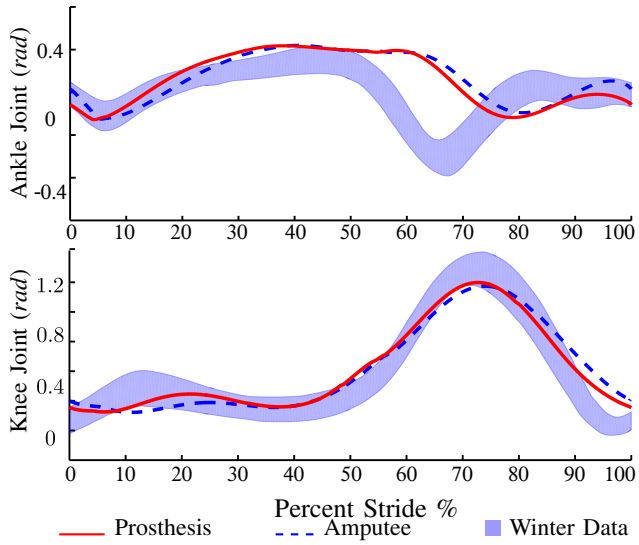

Fig. 4: Trajectory comparisons between the simulated amputee-prosthesis joints and the nominal human locomotion trajectory from Winter data [29].

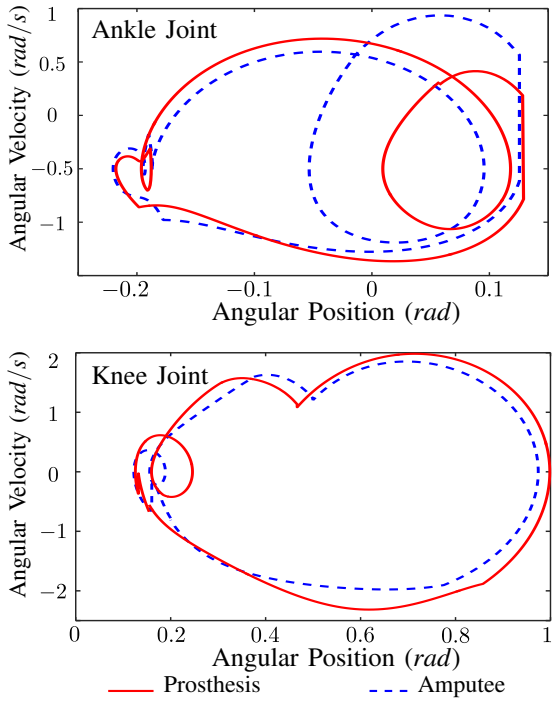

Fig. 5: Phase portraits of the ankle and knee joints of both the amputee and prosthesis over 20 steps.

V. SIMULATION RESULTS

We consider a custom designed 3D prosthetic device in Solidworks as our prosthesis model. The prosthetic leg parameters during the gait design process are obtained from the SolidWorks model. For the ampuee side, we use one of the author's body segment properties as the amputee parameters in simulation. In particular, the shank and foot masses of the amputee are computed to be $3.36kg$ and $1.32kg$ compared to $4.42kg$ and $1.02kg$ of the prosthetic device, respectively. Note that, the inertias for two legs are also different in the model and the total mass of the amputee-prosthesis system is $71kg$.

For the connection force constraints, even though we impose constraints on all three terms of the socket reaction wrenches, the discussion would mainly focus on the z direction force and y direction torque, which are the biggest two terms. Based on research that shows the nominal ground reaction force is about 10 times of the mass of the human, we constrain the z direction force to be smaller than $700N$ and the y direction torque to be smaller than $100Nm$ considering the maximum joint torque. For the other comfortability constraints, we also put particular focus on the z direction impact velocity, which is constrained to be less than $2m/s$. The admissible torques for both the prosthetic ankle joint and knee joint are set to be $120Nm$, which are calculated based on the transmission design of AMPRO3. The joint velocities ($5rad/s$) and position limits ($0 \sim 74$ and $-40 \sim 40$ degree for the knee and ankle joint, respectively) of the prosthetic side are also considered explicitly in the optimization problem.

Results Discussion. The resulting prosthetic trajectories after solving this optimization problem are shown in Fig. 4 with comparisons to both the simulated human side trajectories and the nominal Winter human data [29]. The determinations (R^2) for both gait similarity to unimpaired walking and gait symmetry between the two legs are shown in Table I, which also includes the step size and step velocity for the amputee and prosthesis. As shown in Table I, the prosthesis step is slightly slower with a shorter step size, which is reasonable considering heavier constraints imposed on the prosthetic leg. We also imposed a higher foot clearance constraint for the prosthetic leg to give a bigger safety margin to avoid stumble, which results in a higher maximum flexion for the prosthetic leg as shown in Fig. 4. The resulting gait satisfies the maximum connector wrench constraints. In particular, the maximum z direction force is reduced from $1200N$ (without constraints) to under $700N$. The whole body mechanical CoT of the designed gait is 0.25, which is close to the nominal human locomotion with CoT of 0.2 as reported in [8].

As the PHZD constraints guarantee stability formally, the phase portraits of both the knee and ankle joints for 20 steps are plotted in Fig. 5. Numerical evaluation shows the maximum eigenvalue is $2e^{-4}$, indicating stability of this gait [27]. Gait tiles of two steps are shown in Fig. 6, visually indicated human-likeness of the designed multi-contact gait. A simulation video can be seen in [1] for better illustration of the prosthetic walking from various view angles.

VI. CONCLUSIONS

The authors presented a two-step direct collocation optimization method to formally design 3D multi-contact human-

TABLE I: Performance of Designed Gait.

	Gait (R^2_{ankle},R^2_{knee})		Step		
Stance Leg	Symmetry	Similarity	Clearance	Length	Velocity
Human	(0.96, 0.99)	(0.32, 0.94)	$0.02m$	$0.477m$	$0.515m/s$
Prosthesis	(0.96, 0.99)	(0.41, 0.97)	$0.03m$	$0.476m$	$0.483m/s$

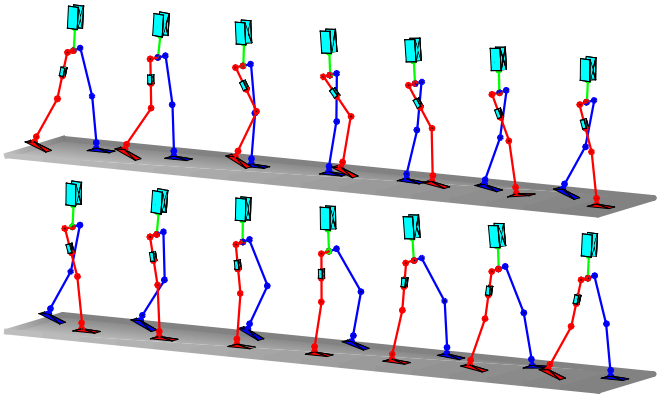

Fig. 6: 3D view of the simulated gaits tiles. Outside leg with red lines is the prosthesis and the rest part represents the amputee. The small blue block on the prosthesis leg represents the connecting socket.

like gaits for prostheses. This goal was achieved by first analyzing special requirements of designing a gait for the asymmetric amputee-prosthesis system. Aiming to systematically embed the human-like multi-contact feature into the gait design process, an 8-domain hybrid system was constructed for the 3D asymmetric robotic model. Combining the prosthetic gait requirements which are imposed as constraints and the hybrid system model, a two-step direct collocation method was proposed with generating a human-like multi-contact prosthesis gait that is both formally stable and physically realizable. Because of the general formulation of this work, the proposed two-step modeling and optimization methods can potentially be applied to design human-like gaits for a wide variety of prostheses.

REFERENCES

[1] Simulation of 3D Multi-Contact Prosthetic Walking. https://youtu.be/eH6NRq1OK3w.

[2] M. Ackermann. *Dynamics and Energetics of Walking with Prostheses*. PhD thesis, University of Stuttgart, Stuttgart, March 2007.

[3] A. D. Ames. Human-inspired control of bipedal walking robots. *Automatic Control, IEEE Transactions on*, 59(5):1115–1130, 2014.

[4] A. D. Ames, K. Galloway, K. Sreenath, and J. W. Grizzle. Rapidly exponentially stabilizing control Lyapunov functions and hybrid zero dynamics. *Automatic Control, IEEE Transactions on*, 59(4):876–891, 2014.

[5] A. D. Ames, R. Vasudevan, and R. Bajcsy. Human-data based cost of bipedal robotic walking. In *Hybrid Systems: Computation and Control*, pages 153–162, Chicago, IL, 2011.

[6] S. Au, M. Berniker, and H. Herr. Powered ankle-foot prosthesis to assist level-ground and stair-descent gaits. *Neural Networks*, 21(4):654 – 666, 2008.

[7] V. Azimi, D. Simon, H. Richter, and S. A. Fakoorian. Robust composite adaptive transfemoral prosthesis control with non-scalar boundary layer trajectories. In *American Control Conference (ACC)*, July 2016.

[8] S. H. Collins and A. Ruina. A bipedal walking robot with efficient and human-like gait. In *Robotics and Automation, 2005. ICRA 2005. Proceedings of the 2005 IEEE International Conference on*, pages 1983–1988, April 2005.

[9] T. Dillingham. Limb amputation and limb deficiency: Epidemiology and recent trends in the united states. *Southern Medical Journal*, 2002.

[10] W. C. Flowers and R. W. Mann. Electrohydraulic knee-torque controller for a prosthesis simulator. *ASME J. of Biomechanical Engineering*, 99(no.4):pp.3–8, 1977.

[11] R. D. Gregg, T. Lenzi, L. J. Hargrove, and J. W. Sensinger. Virtual constraint control of a powered prosthetic leg: From simulation to experiments with transfemoral amputees. *Robotics, IEEE Transactions on*, 30(6):1455–1471, Dec 2014.

[12] J. W. Grizzle, C. Chevallereau, R. W. Sinnet, and A. D. Ames. Models, feedback control, and open problems of 3D bipedal robotic walking. *Automatica*, 50(8):1955 – 1988, 2014.

[13] A. Gunnar and L. Peterson. Effects of shoe and surface characteristics on lower limb injuries in sports. *Journal of Applied Biomechanics*, 2(3):202 – 9, 1986.

[14] K. A. Hamed and R. D. Gregg. Decentralized feedback controllers for exponential stabilization of hybrid periodic orbits: Application to robotic walking*. In *American Control Conference*, Boston, 2016.

[15] A. Hereid, E. A. Cousineau, C. M. Hubicki, and A. D. Ames. 3D dynamic walking with underactuated humanoid robots: A direct collocation framework for optimizing hybrid zero dynamics. In *IEEE International Conference on Robotics and Automation (ICRA)*, pages 1447–1454. IEEE, 2016.

[16] K. W. Hollander and T. G. Sugar. A robust control concept for robotic ankle gait assistance. In *Rehabilitation Robotics, ICORR, IEEE 10th International Conference on*, pages 119–123, 2007.

[17] V. T. Inman and J. Hanson. Human locomotion. In *Human Walking*. Williams & Wilkins, Baltimore, 1994.

[18] SM. Jaegers, JH. Arendzen, and HJ. de Jongh. Prosthetic gait of unilateral transfemoral amputees: a kinematic study. *Archives of physical medicine and rehabilitation*, 76(8):736–743, 1995.

[19] D. C. Morgenroth, A. D. Segal, K. E. Zelik, J. M. Czerniecki, G. K. Klute, P. G. Adamczyk, M. S. Orendurff, M. E. Hahn, S. H. Collins, and A. D. Kuo. The effect of prosthetic foot push-off on mechanical loading associated with knee osteoarthritis in lower extremity amputees. *Gait & posture*, 34(4):502–507, 2011.

[20] R. M. Murray, Z. Li, and S. S. Sastry. *A Mathematical Introduction to Robotic Manipulation*. CRC Press, Boca Raton, March 1994.

[21] A. M. Oymagil, J. K. Hitt, T. Sugar, and J. Fleeger. Control of a regenerative braking powered ankle foot orthosis. In *Rehabilitation Robotics, IEEE 10th International Conference on*, pages 28–34, 2007.

[22] D. Popovic, R. Tomovic, D. Tepavac, and L. Schwirtlich. Control aspects of active above-knee prosthesis. *International Journal of Man-Machine Studies*, 35(6):751 – 767, 1991.

[23] S. S. Sastry. *Nonlinear Systems: Analysis, Stability and Control*. Springer, New York, June 1999.

[24] A. M. Simon, K. A. Ingraham, N. P. Fey, S. B. Finucane, R. D. Lipschutz, A. J. Young, and L. J. Hargrove. Configuring a powered knee and ankle prosthesis for transfemoral amputees within five specific ambulation modes. *PloS one*, 9(6):e99387, 2014.

[25] F. Sup, A. Bohara, and M. Goldfarb. Design and control of a powered transfemoral prosthesis. *The International journal of robotics research*, 27(2):263–273, February 2008.

[26] M. R Tucker, . Olivier, A. Pagel, H. Bleuler, M. Bouri, O. Lambercy, J. del R Millán, R. Riener, H. Vallery, and R. Gassert. Control strategies for active lower extremity prosthetics and orthotics: a review. *Journal of neuroengineering and rehabilitation*, 12(1):1, 2015.

[27] E. D. B. Wendel and A. D. Ames. Rank properties of Poincaré maps for hybrid systems with applications to bipedal walking. In *Hybrid Systems: Computation and Control*, pages 151–60, Stockholm, 2010.

[28] E. R. Westervelt, J. W. Grizzle, C. Chevallereau, J. H. Choi, and B. Morris. *Feedback Control of Dynamic Bipedal Robot Locomotion*. CRC Press, Boca Raton, June 2007.

[29] D. A. Winter. *Biomechanics and Motor Control of Human Movement*. Wiley-Interscience, New York, 2 edition, May 1990.

[30] H. Zhao, A. Hereid, W-L Ma, and A. D Ames. Multi-contact bipedal robotic locomotion. *Robotica*, pages 1–35.

[31] H. Zhao, J. Horn, J. Reher, V. Paredes, and A. D. Ames. A hybrid systems and optimization-based control approach to realizing multi-contact locomotion on transfemoral prostheses. *IEEE Transactions on Automation Science and Engineering*, Jan 2016.

[32] H. Zhao, M. J. Powell, and A. D. Ames. Human-inspired motion primitives and transitions for bipedal robotic locomotion in diverse terrain. *Optimal Control Applications and Methods*, 35(6):730–755, 2014.

[33] H. Zhao, J. Reher, J. Horn, V. Paredes, and A. D. Ames. Realization of stair ascent and motion transitions on prostheses utilizing optimization-based control and intent recognition. In *Rehabilitation Robotics (ICORR), IEEE International Conference on*, pages 265–270, 2015.